OPEN
Original article

Nuclear Medicine Communications

CD133 increases oxidative glucose metabolism of HT29 cancer cells by mitochondrial uncoupling and its inhibition enhances reactive oxygen species-inducing therapy

Jin Hee Lee[a,b], Eun Ji Lee[a], Jin Won Park[c], Mina Kim[a], Kyung-Ho Jung[a,b], Young Seok Cho[a] and Kyung-Han Lee[a,b]

Objective **A better understanding of the metabolic phenotype of stem-like cancer cells could provide targets to help overcome chemoresistance. In this study, we hypothesized that colon cancer cells with the stem cell feature of CD133 expression have increased proton leakage that influences glucose metabolism and offers protection against reactive oxygen species (ROS)-inducing treatment.**

Methods and Results **In HT29 colon cancer cells, ^{18}F-fluorodeoxyglucose (FDG) uptake was increased by CD133 selection and decreased by CD133 silencing. In CD133(+) cells, greater ^{18}F-FDG uptake was accompanied by increased oxygen consumption rate (OCR) and reduced mitochondrial membrane potential and mitochondrial ROS, indicating increased proton leakage. The uncoupling protein inhibitor genipin reversed the increased ^{18}F-FDG uptake and greater OCR of CD133(+) cells. The ROS-inducing drug, piperlongumine, suppressed CD133(−) cell survival by stimulating mitochondrial ROS generation but was unable to influence CD133(+) cells when used alone. However, cotreatment of CD133(+) cells with genipin and piperlongumine efficiently stimulated mitochondrial ROS for an enhanced antitumor effect with substantially reduced CD133 expression.**

Conclusion **These results demonstrate that mitochondrial uncoupling is a metabolic feature of CD133(+) colon cancer cells that provides protection against piperlongumine therapy by suppressing mitochondrial ROS generation. Hence, combining genipin with ROS-inducing treatment may be an effective strategy to reverse the metabolic feature and eliminate stem-like colon cancer cells.** *Nucl Med Commun* **43: 937–944**

Nuclear Medicine Communications 2022, **43**:937–944

Keywords: CD133, colon cancer, glucose, oxygen consumption rate, mitochondrial reactive oxygen species

[a]Department of Nuclear Medicine, Samsung Medical Center, [b]Department of Health Sciences and Technology, SAIHST, Sungkyunkwan University School of Medicine, Seoul and [c]Scripps Korea Antibody Institute, Chuncheon-si, South Korea

Correspondence to Kyung-Han Lee, MD, PhD, Department of Nuclear Medicine, Samsung Medical Center, 50, Irwon-dong, Gangnam-gu, Seoul 135-710, South Korea
Tel: +82 2 3410 2630; fax: +82 2 3410 2638; e-mail: khleenm@naver.com

Received 9 December 2021 **Accepted** 28 April 2022

Introduction

Cancer chemoresistance is attributed to cancer stem cells (CSCs) that are responsible for tumor recurrence and metastasis [1]. The metabolic phenotype of CSCs may contribute to chemoresistance by offering survival advantage against oxidative stress. Proliferating cancer cells are recognized to have heightened glucose utilization [2], and the metabolic phenotype of cancers including that of colorectal tumors is assessed by clinical PET with ^{18}F-fluorodeoxyglucose (^{18}F-FDG) [3]. However, tumor cells are heterogeneous in metabolic feature, with distinct metabolic programs activated for different subpopulations. Despite growing interest in therapeutic targeting of CSC metabolism [4], our understanding of their bioenergetic adaptation remains incomplete. Several CSCs were observed to be more glycolysis-dependent than differentiated cancer cells [5,6], whereas other CSCs have shown a preference for mitochondrial oxidative respiration [7,8].

Metabolic rewiring of cancer cells is closely connected to redox status, which influences their differentiation and survival. In CSCs, reactive oxygen species (ROS) is fine-tuned below a certain threshold to maintain stemness features [9,10], and excessive mitochondrial ROS could cause detrimental insult. A key regulator of oxidative redox generation is mitochondrial uncoupling that downregulates ROS generation by inducing proton leakage from the inner membrane [11,12]. This raises the potential for a role of mitochondrial uncoupling in the metabolic and redox characteristics of CSCs. Because protection from oxidative stress can promote chemotherapy resistance [13–15], a

Supplemental Digital Content is available for this article. Direct URL citations appear in the printed text and are provided in the HTML and PDF versions of this article on the journal's website, www.nuclearmedicinecomm.com.

better understanding of the metabolic phenotype of colon CSCs may help open new therapeutic windows.

CSCs are recognized by specific cell surface markers, and cluster of differentiation (CD)133 is a transmembrane glycoprotein widely used for CSC identification and selection [16]. In colon cancer, CD133(+) CSCs mediate tumor growth and metastatic dissemination [17,18]. CD133 expression has been associated with greater treatment resistance, but the potential involvement of glucose metabolism and oxidative stress remains unclear. In this study, we hypothesized that CD133(+) colon cancer cells have increased mitochondrial oxidative metabolism by proton leak respiration that provides protection against mitochondrial ROS. We further investigated whether the natural uncoupling protein-2 (UCP2) inhibitor, genipin, could overcome this metabolic feature and enhance the antitumor effect of ROS-inducing therapy.

Materials and methods

Cell culture and reagents

HT29 and HCT116 human colon cancer cells from the American Type Culture Collection (Manassas, Virginia, USA) were maintained in Roswell Park Memorial Institute (RPMI) media supplemented with 10% fetal bovine serum (FBS) (Serana, Germany) and 1% penicillin/streptomycin at 37 °C and 5% CO_2 in a humidified atmosphere. Cells were subcultured twice a week and used at passages less than 10 when confluence reached 80%. Cells were authenticated and confirmed mycoplasma-free by the institutional research support center.

RPMI medium, Hanks' Balanced Salt Solution (HBSS) buffer, phenol red-free RPMI, and penicillin/streptomycin were from Gibco Laboratories (Gaithersburg, Maryland, USA). Genipin was from Sigma-Aldrich (St. Louis, Missouri, USA), piperlongumine was from Merck (Darmstadt, Germany), and CM-H2DCFDA [5-(and-6)-chloromethyl-2′, 7′-dichlorodihydrofluorescein diacetate acetyl ester] was from Invitrogen (Carlsbad, California, USA). MitoSOX Red, mitotracker Red FM, lipofectamine RNAiMax reagent, opti-MEM, and anti-β-actin IgG (cat. no. 18470) were from Thermo Fisher Scientific (Waltham, Massachusetts, USA). Anti-CD133 IgG was from Proteintech, Rosemont, Illinois (cat. no. 18470-I-AP); PE-tagged anti-CD133 IgG (cat. no. 130-090-853) was from Miltenyi Biotec; anti-UCP2 antibody (cat. no. 89326), horseradish peroxidase–linked secondary antirabbit (cat. no. 7074), and antimouse IgG (cat. no. 7076) were from Cell Signaling Technology (Danvers, Massachusetts, USA).

^{18}F-fluorodeoxyglucose uptake measurement

Cells were seeded onto 24-well plates at a density of 1×10^5 cells/well. On the day of experiments, the ^{18}F-FDG uptake was conducted as previously described [19].

Lactate production assay

To quantify lactate secretion, CD133(+) and CD133(−) cells sorted by fluorescence-activated cell sorting (FACS) analysis were seeded onto 24-well plates in normal culture medium at densities of 1×10^5 cells per well. After 48 h of incubation without media change, 0.5 ml of culture media was removed from each well and underwent L-lactate measurement using a Cobas assay kit (Roche Diagnostics, Basel, Switzerland) following the manufacturer's instructions as previously described [20]. The lactate in each sample began accumulating from secretion by 1×10^5 cells at seeding, but based on HT29 cell doubling time and protein assays at the time of collection, cell number is estimated to have reached approximately 3×10^5 after 48 h.

Oxygen consumption rate and extracellular acidification rate measurements

For oxygen consumption rate (OCR) measurement, cells were seeded onto a Seahorse analyzer plate (Seahorse Bioscience North Billerica,Massachusetts, USA) at a density of 5×10^4 cells/well in 100 µl of RPMI culture medium containing 1 g/l of glucose. Cellular OCR was measured by the Seahorse XF24 software version 1.8 as previously described [20]. For extracellular acidification rate (ECAR) measurement, cells were seeded onto a Seahorse analyzer plate as above, but in 100 µl of glucose-free RPMI medium. The medium was change to RPMI containing 1 g/l of glucose before ECAR measurement.

CD133 silencing with specific small interfering RNA

CD133-specific small interfering RNA (siRNA) (Thermo Fisher Scientific) consisted of 20–25 target-specific nucleotides to knock down CD133 gene expression. Nontargeting scrambled siRNA was used as a control. Transfection was performed following previously described [19].

Fluorescence-activated cell sorting for CD133 expression

FACS sorting for CD133 expression was performed by incubating 20×10^6 cells with PE-tagged anti-CD133 antibody (1:200) for 30 min at 37 °C. Sorting was performed on an Aria cell sorter (BD Biosciences, San Diego, California, USA) using a 488-nm laser excitation channel and a 575-nm fluorescent emission channel. Sorted cells were seeded and maintained in culture media until experiments.

Total cellular reactive oxygen species and mitochondrial reactive oxygen species measurements

A total of 2×10^4 cells were seeded per well into a black 96-well plate with a transparent bottom in 10% FBS-containing phenol red-free RPMI. Intracellular ROS levels were quantified using the cell-permeant indicator CM-H2DCFDA as previously described [19].

Mitochondrial ROS was measured by flow cytometry. Briefly, 5×10^5 cells seeded per well into six-well plates were removed from medium and replaced with HBSS buffer containing Ca/Mg, 2% BSA, and 5 μmol/l of MitoSOX dye. Cells were washed with PBS 30 min later, collected by trypsinization, and washed with HBSS buffer containing Ca/Mg and 2% BSA. After centrifugation, cells were suspended with the same buffer and transferred to a sterile cell strainer tube. Flow cytometric measurement of mitochondrial ROS was carried out on a FACS Calibur (BD Bioscience) with CellQuest software (Becton-Dickinson, Franklin Lakes, New Jersey, USA) with data collection in the forward scatter, side scatter, and the fluorescence 2 channels.

Mitochondrial membrane potential measurement

At 24 h after 2×10^4 cells were seeded per well into a 96-well plate, culture media was replaced with phenol red-free RPMI containing 2% FBS and 0.5 μmol/l of MitoTracker Red FM. The measurement of mitochondrial membrane potential (MMP) was done as previously described [19].

Sulforhodamine B assay

For survival assays, 2×10^4 cells were seeded per well into a 96-well plate. After 48 h of treatment, sulforhodamine B assay was conducted as previously described [19].

Immunoblotting for CD133 and uncoupling protein-2 expression

Immunoblotting was performed as previously described [19]. The primary antibodies against CD133 (1:2000 dilution), UCP2 (1:1000 dilution), or β-actin (1: 5000 dilution) were used.

Statistical analysis

Data are presented as mean ± SD. Significant differences between groups were analyzed by paired Student's *t*-tests. *P*-values < 0.05 were considered statistically significant.

Results

Effect of CD133 expression on glucose uptake in HT29 colon cancer cells

HT29 human colon cancer cells were first tested after transfection with CD133-specific siRNA. This effectively silenced the CD133 protein level to 18.7 ± 1.8% of untreated cells and 21.3 ± 2.1% of control cells transfected with scrambled siRNA (both $P < 0.001$; Fig. 1a). Silencing of CD133 expression significantly reduced the uptake of ^{18}F-FDG to 75.6 ± 5.8% of scrambled siRNA controls ($P < 0.005$; Fig. 1a).

We next separated HT29 cells according to CD133 expression by FACS sorting. Western blots confirmed strong CD133 expression in CD133(+) cells that was 4.9 ± 0.4-fold that found among CD133(–) cells ($P < 0.005$) (Fig. 1b). CD133(+) cells displayed significantly greater ^{18}F-FDG uptake that reached 207.6 ± 16.1% of CD133(–) cells ($P < 0.001$; Fig. 1c). However, there was no difference in lactate production (Fig. 1c), indicating that the extra glucose taken up was not used for glycolysis.

CD133(+) HCT116 human colon cancer cells also showed significantly greater ^{18}F-FDG uptake that reached 165.8 ± 4.2% of that for CD133(–) cells ($P < 0.001$; Supplementary Fig. 1, supplemental digital content 1, *http://links.lww.com/NMC/A220*).

Mitochondrial oxidative respiration and extracellular acidification rate according to CD133 expression

Extracellular flux analysis revealed that CD133(+) cells have significantly greater baseline OCR that reached 166.1 ± 11.8% of that for CD133(–) cells ($P < 0.001$) (Fig. 2a). This illustrates an association of higher glucose uptake with mitochondrial oxidative metabolism. Notably, OCR in CD133(+) cells was also greater in the presence of the complex V inhibitor oligomycin (149.6 ± 28.8% of CD133(–) cells; $P < 0.05$; Fig. 2a), which revealed increased proton leak respiration. Furthermore, CD133(+) cells showed greater maximal respiratory capacity (140.8 ± 13.8% of CD133(–) cells; $P < 0.005$) when the protonophore trifluoromethoxy carbonylcyanide phenylhydrazone (FCCP) was added (Fig. 2a).

In comparison, ECAR measurements were not significantly different for CD133(–) and CD133(+) cells at baseline as well as after addition of oligomycin and FCCP (Fig. 2a).

Effects of genipin on HT29 cell glucose metabolism

The extracellular flux analysis results prompted us to explore the possible involvement of mitochondrial respiratory uncoupling. When cells were treated with the widely used uncoupling inhibitor, genipin, CD133(+) cells completely lost the 4.4 ± 0.3-fold greater ^{18}F-FDG uptake that was present without treatment ($P < 0.001$) (Fig. 2b). Genipin treatment also significantly reduced the basal OCR of CD133(+) cells that had been increased to 251 ± 25% of CD133(–) cells (Fig. 2b).

Whereas lactate release was similar between untreated CD133(+) and CD133(–) cells (97.6 ± 1.5% vs. 100.0 ± 0.9%), genipin significantly decreased lactate production in both groups of cells to 82.0 ± 1.0% and 78.9 ± 3.4% of untreated CD133(–) control level, respectively, (both $P < 0.001$; Fig. 2b). ECAR measurements confirmed consistent results by showing that genipin treatment caused 53.5 ± 2.6% and 32.0 ± 6.0% reductions in acidification rate for CD133(–) cells and CD133(+) cells, respectively (Fig. 2b).

Mitochondrial membrane potential and reactive oxygen species production of cells according to C133 expression

Although western blotting did not show a difference in UCP2 protein level between CD133(–) and CD133(+) cells (Fig. 3a), the function of the protein is commonly

Fig. 1

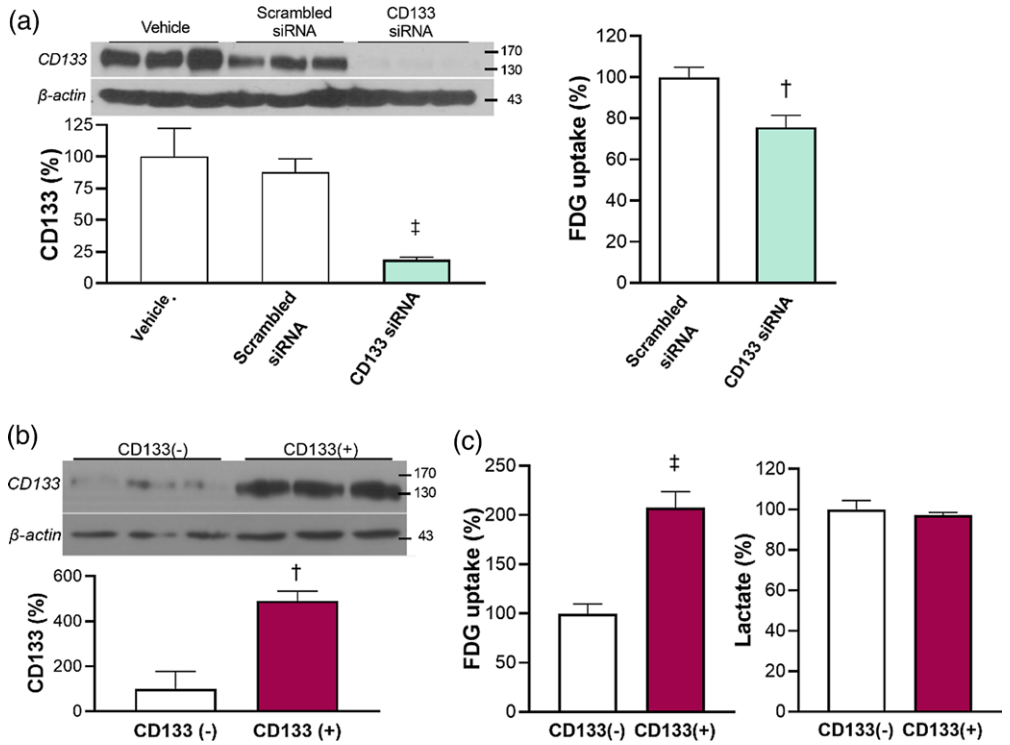

Glucose metabolism of HT29 colon cancer cells according to CD133 expression. (a) Effect of CD133 silencing with specific siRNA on CD133 protein level (left) and ^{18}F-FDG uptake (right). (b and c) Comparison of CD133 expression (b), and ^{18}F-FDG uptake and lactate production (c) in CD133(+) and CD133(–) cells sorted by flow cytometry. Sorted cells were cultured for 48 h in 10% FBS-containing 1g/l of glucose RPMI medium before experiments. Statistical analysis was performed by paired Student's *t*-tests. All bars are mean ± SD of % relative to CD133(–) cells of triplicate samples obtained from a single representative experiment. $^{\dagger}P < 0.005$, $^{\ddagger}P < 0.001$ vs. controls (a) or CD133(–) cells (b and c). RPMI, Roswell Park Memorial Institute.

activated without change in amount [20–24]. Such activation is characterized by lowered MMP and reduced ROS production. Assessment of these properties confirmed significantly lower MMP for CD133(+) cells at 82.8 ± 2.0% of CD133(–) cells ($P < 0.001$; Fig. 3b). CD133(+) cells also had significantly lower mitochondrial ROS production that was reduced to 70.8 ± 3.8% of CD133(–) cells ($P < 0.001$; Fig. 3c). Total cellular ROS was not significantly different between the two groups of cells.

Effects of piperlongumine and genipin on HT29 cell survival

We next compared the capacity of piperlongumine to suppress HT29 cell survival when used alone or in combination with genipin. Treatment with 10 μmol/l of piperlongumine alone for 48 h modestly suppressed the survival of CD133(–) cells but not CD133(+) cells ($P < 0.001$) (Fig. 4a). Treatment with 250 μmol/l of genipin alone for 48 h suppressed the survival of CD133(–) cells to 76.9 ± 7.1% of controls but again did not affect the survival of CD133(+) cells ($P < 0.001$) (Fig. 4a).

In CD133(–) cells, combination therapy with piperlongumine plus genipin for 48 h caused additive antitumor effects, leading to 67.5 ± 1.6% and 58.9 ± 2.5% survival, respectively (Fig. 4a). In CD133(+) cells, combination therapy resulted in an enhanced antitumor effect. This substantially reduced cell survival to 52.9 ± 0.7% of controls, which was even lower than that of CD133(–) cells ($P = 0.003$) (Fig. 4a).

Effects of piperlongumine and genipin on mitochondrial reactive oxygen species

To assess the mechanism of the enhanced antitumor effect, mitochondrial ROS was measured following treatment with piperlongumine and/or genipin for 48 h. In CD133(–) cells, 10 μmol/l of piperlongumine and 250 μmol/l of genipin alone substantially increased the mitochondrial ROS to 181.2 ± 20.4% and 304.9 ± 6.5% of vehicle-treated controls, respectively (Fig. 4b). In CD133(+) cells, however, piperlongumine alone was unable to increase mitochondrial ROS (Fig. 4b). Genipin increased CD133(+) cell mitochondrial ROS both alone [213.8 ± 25.5%; $P < 0.05$ vs. CD133(–) cells] and in combination with piperlongumine (Fig. 4b). Notably, mitochondrial ROS reached similarly high levels in CD133(–)

Fig. 2

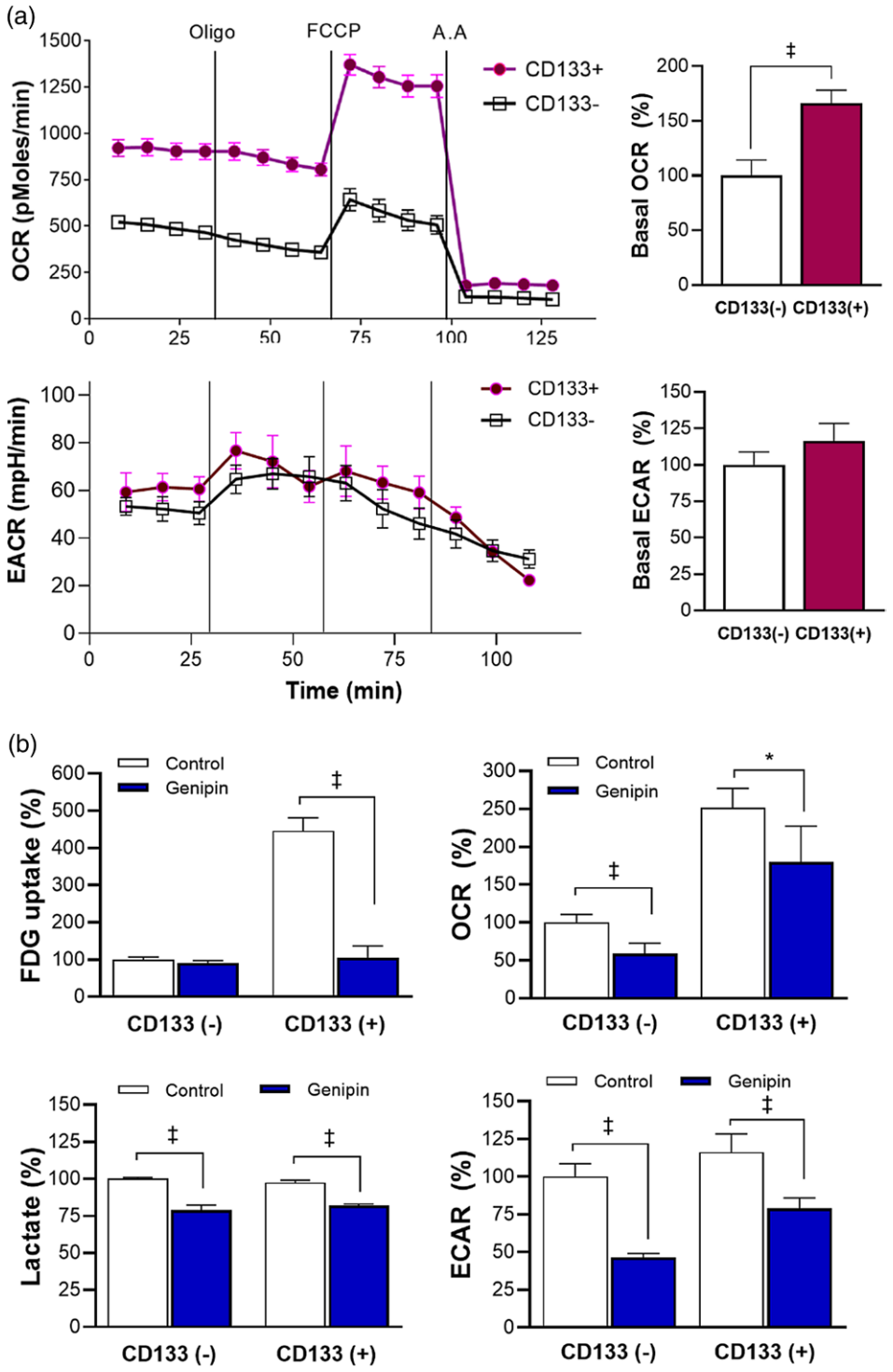

Mitochondrial oxidative respiration and acid generation. (a) OCR (top) and ECAR (bottom) in CD133(+) and CD133(–) HT29 cells at baseline and after sequential addition of oligomycin (oligo; complex V inhibitor) to derive ATP-linked and proton leak respiration, FCCP (protonophore) to collapse the inner membrane gradient and derive maximal respiratory capacity, and antimycin A (A.A; complex III inhibitor) to shut down ETC function and reveal nonmitochondrial respiration. Basal OCR and ECAR levels are shown in the right. (b) Metabolic effects of genipin on CD133(+) and CD133(–) HT29 cells. Comparison of ^{18}F-FDG uptake (top left), baseline OCR (top right), lactate production (bottom left), and baseline ECAR (bottom right) in cells treated with vehicle or the UCP2 inhibitor genipin (250 μmol/l) for 48 h. All data are mean ± SD, and all bars are % relative to untreated CD133(–) cells of quadruplicate (OCR and ECAR) or triplicate (^{18}F-FDG uptake and lactate) samples obtained from a single representative experiment. $^{*}P < 0.06$; $^{**}P < 0.01$; $^{‡}P < 0.001$. FCCP, trifluoromethoxy carbonylcyanide phenylhydrazone.

Fig. 3

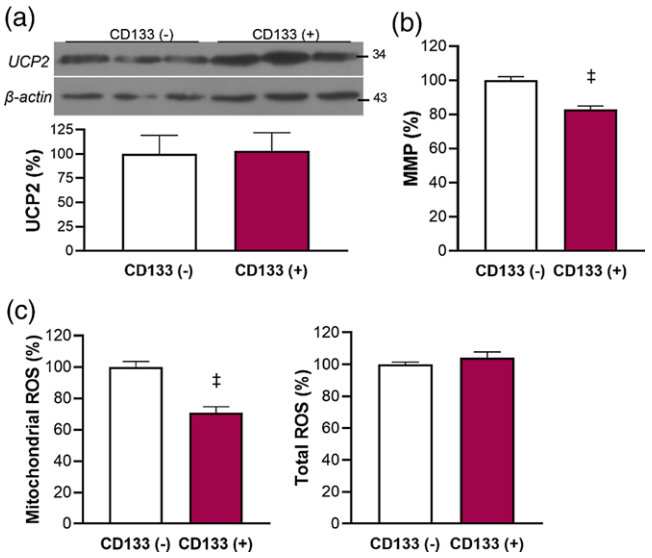

MMP and ROS production according to CD133 expression. (a) Western blots and quantified band intensities of UCP2 protein. (b) Comparison of MMP of CD133(–) and CD133(+) cells sorted by flow cytometry. (c) Mitochondrial ROS (left) and total cellular ROS production (right) in CD133(–) and CD133(+) cells. Sorted cells were cultured for 48 h in RPMI medium containing 10% FBS before experiments. Statistical analysis was performed by paired Student's *t*-tests. All bars are mean ± SD of % relative to CD133(–) cells of triplicate (a) or quadruplicate samples (b and c) obtained from a single representative experiment. $^{‡}P < 0.001$. RPMI, Roswell Park Memorial Institute.

cells (398.8 ± 4.5%) and CD133(+) cells (392.7 ± 7.3%) following combination therapy (Fig. 4b).

Effects of piperlongumine and genipin on CD133 and uncoupling protein-2 expression

Finally, the effects of piperlongumine and/or genipin on CD133 expression were evaluated. In CD133(+) cells, CD133 protein bands that were strong at baseline modestly decreased after treatment with piperlongumine or genipin alone (76.9 ± 15.2% and 63.8 ± 12.4% of controls, respectively). Combined piperlongumine plus genipin substantially suppressed CD133 expression to 24.2 ± 0.8% of untreated controls ($P < 0.001$) (Fig. 4c). In CD133(–) cells, CD133 protein bands that were weak at baseline remained faint after the treatments (Fig. 4c).

Piperlongumine and genipin did not influence UCP2 expression level in either group of cells (Fig. 4d).

Discussion

This study demonstrates elevated ^{18}F-FDG uptake in HT29 colon cancer cells that express CD133 compared with cells that do not. The increased glucose taken up was utilized for mitochondrial oxidative respiration rather than glycolytic flux. A preference for oxidative metabolism can be considered consistent with the quiescent behavior of CSCs as compared with rapidly proliferating cancer cells.

Extracellular flux analysis confirmed that CD133(+) HT29 cells had greater baseline and maximal OCR, consistent with a more active electron transport chain process. Importantly, the cells had an elevated level of proton leak respiration as shown by greater OCR in the presence of the complex V inhibitor oligomycin [20,22]. These results reveal that CD133-positive HT29 cancer cells have increased ^{18}F-FDG uptake by an elevated oxygen consumption rate, which is attributable to mitochondrial uncoupling.

Mitochondrial uncoupling through anion carrier proteins dissipate MMP by facilitating free reentry of protons from the outer to inner mitochondrial membrane without energy production [11,12]. Although CD133(+) cells did not show significantly increased UCP2 protein content, this is consistent with the notion that proton leakage is typically modulated by changes in functional activity rather than the amount of UCP2 protein [19–21]. Greater uncoupling activity in CD133(+) cells was evidenced by lower MMP, which is dependent on intermembrane proton buildup and is therefore reduced by proton leakage. The cells also had lower mitochondrial ROS despite greater OCR. Lower MMP and ROS were previously observed in CSCs derived from oral and skin carcinomas [23]. Mitochondrial ROS production during the escape of electrons from the electron transport complex is highly sensitive to mild uncoupling activity [24,25]. Lower MMP and ROS levels in CD133(+) HT29 cells, therefore, support greater uncoupling activity.

Fig. 4

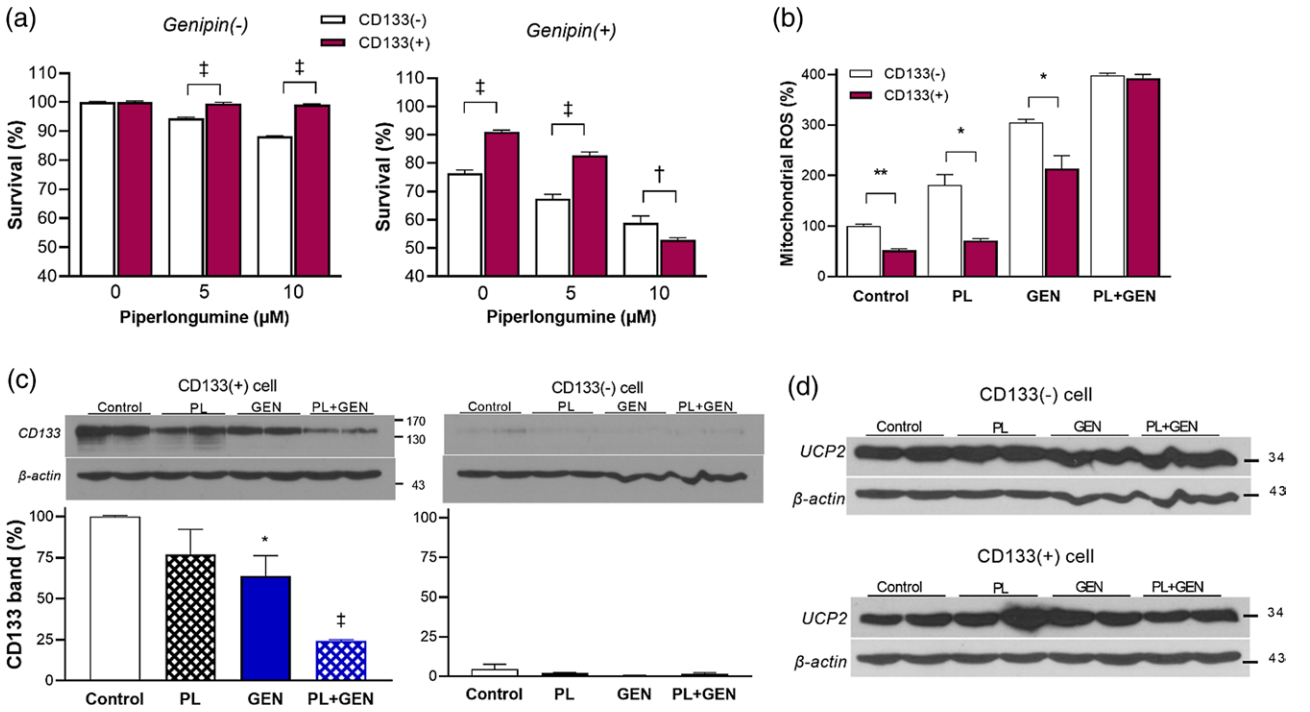

Genipin (GEN) enhances the antitumor effect of piperlongumine (PL) by augmenting mitochondrial ROS. The effects of GEN and PL on CD133, UCP2 expression. (a) Surviving fractions of CD133(–) and CD133(+) HT29 cells after 48 h of treatment with 0, 5, or 10 μmol/l of PL in the absence (left) or presence of 250 μmol/l of GEN (right). (b) Mitochondrial ROS in CD133(–) and CD133(+) HT29 cells after 48 h of treatment with 10 μmol/l of PL and/or 250 μmol/l of GEN. Statistical analysis was performed by paired Student's *t*-tests. Bars are mean ± SD of % of vehicle-treated controls of quadruplicate (a) or duplicate samples (b) obtained from a single representative experiment. (c) Western blot and quantified band intensities of the CD133 protein in CD133(+) (left) and CD133(–) cells (right) after treatment. Statistical analysis was performed by paired Student's *t*-tests. Bars are mean ± SD of % relative to untreated CD133(+) cells of duplicate samples obtained from a single representative experiment. $^{*}P < 0.05$, $^{**}P < 0.01$, $^{\dagger}P < 0.005$, $^{\ddagger}P < 0.001$. (D) Western blotting and quantified band intensities of UCP2 protein in CD133(–) (top) and CD133(+) cells (bottom) after treatment as above.

Further evidence for the role of uncoupling activity on the metabolic phenotype of CD133(+) cells was provided by the natural uncoupling inhibitor, genipin [18,19]. We found that genipin completely canceled the greater ^{18}F-FDG uptake and substantially reduced the elevated oxygen consumption observed in untreated CD133(+) cells. By blocking dissipation of mitochondrial proton gradient, genipin can reduce energy expenditure and, thus, glucose requirement. Therefore, the ability of genipin to reverse the metabolic phenotype of CD133(+) cells demonstrates the contribution of uncoupling activity.

Cancer cells require redox homeostasis for survival and are susceptible to ROS increased over the cytotoxic threshold. This is the basis for the strategy of using ROS-inducing agents for cancer therapy. However, cancer cells may devise ways to protect against unfavorable redox conditions [26], and the metabolic property of CSCs may help to prevent excessive ROS accumulation. We therefore compared the therapeutic effects of piperlongumine, a small ROS-inducing molecule that has powerful cancer cell-selective killing properties [27], in CD133(–) and CD133(+) cells.

Our results showed that, whereas piperlongumine increased mitochondrial ROS in CD133(–) cells, it did not do so in CD133(+) cells. In comparison, genipin alone increased the mitochondrial ROS in both CD133(–) and CD133(+) cells. Similar ROS-stimulating effects of genipin have been previously observed in various types of cancer cells [12,21,22], and this is consistent with its ability to block MMP dissipation. When piperlongumine and genipin were combined, mitochondrial ROS was substantially increased in both CD133(–) and CD133(+) cells to comparable levels. Importantly, CD133(+) cells were resistant to treatment with piperlongumine alone but were efficiently eliminated when genipin was added. These findings are consistent with the notion that mild proton leakage provides a first line of protection against oxidative stress [28] and that inhibition of mitochondrial uncoupling can reverse this action [29].

Interestingly, combining piperlongumine and genipin substantially reduced CD133 expression in CD133(+) cells. Certain drugs have shown the capacity to modulate cancer cell CD133 expression. For example, thalidomide downregulated CD133 expression in pancreatic

cancer cells [30], whereas oxytetracycline did so in liver CSCs [31]. In addition, metformin decreased CD133 expression in liver cancer cells through AMP-activated protein kinase signaling [32]. Our results likely represent an example of the preferential killing of cells with high CD133 expression by blocking the protective effect of mitochondrial uncoupling. Since failure to eradicate CSCs is a cause of cancer recurrence, this points to the potential benefit of combining ROS-inducing agents with mitochondrial uncoupling inhibitors to eliminate colon cancer cells with stemness properties.

Acknowledgements

This study was supported by the Basic Science Research Program through the National Research Foundation of Korea (NRF) funded by the Ministry of Science, ICT and Future Planning (NRF-2019R1A2C2007455).

Conflicts of interest

There are no conflicts of interest.

References

1 Batlle E, Clevers H. Cancer stem cells revisited. *Nat Med* 2017; **23**:1124–1134.
2 Hanahan D, Weinberg RA. Hallmarks of cancer: the next generation. *Cell* 2011; **144**:646–674.
3 Goh V, Engledow A, Rodriguez-Justo M, Shastry M, Peck J, Blackman G, *et al*. The flow-metabolic phenotype of primary colorectal cancer: assessment by integrated 18F-FDG PET/perfusion CT with histopathologic correlation. *J Nucl Med* 2012; **53**:687–692.
4 Jones CL, Inguva A, Jordan CT. Targeting energy metabolism in cancer stem cells: progress and challenges in leukemia and solid tumors. *Cell Stem Cell* 2021; **28**:378–393.
5 Palorini R, Votta G, Balestrieri C, Monestiroli A, Olivieri S, Vento R, Chiaradonna F. Energy metabolism characterization of a novel cancer stem cell-like line 3AB-OS. *J Cell Biochem* 2014; **115**:368–379.
6 Zhou Y, Zhou Y, Shingu T, Feng L, Chen Z, Ogasawara M, *et al*. Metabolic alterations in highly tumorigenic glioblastoma cells: preference for hypoxia and high dependency on glycolysis. *J Biol Chem* 2011; **286**:32843–32853.
7 Sancho P, Burgos-Ramos E, Tavera A, Bou Kheir T, Jagust P, Schoenhals M, *et al*. MYC/PGC-1α balance determines the metabolic phenotype and plasticity of pancreatic cancer stem cells. *Cell Metab* 2015; **22**:590–605.
8 Vlashi E, Lagadec C, Vergnes L, Reue K, Frohnen P, Chan M, *et al*. Metabolic differences in breast cancer stem cells and differentiated progeny. *Breast Cancer Res Treat* 2014; **146**:525–534.
9 Porporato PE, Payen VL, Pérez-Escuredo J, De Saedeleer CJ, Danhier P, Copetti T, *et al*. A mitochondrial switch promotes tumor metastasis. *Cell Rep* 2014; **8**:754–766.
10 Piskounova E, Agathocleous M, Murphy MM, Hu Z, Huddlestun SE, Zhao Z, *et al*. Oxidative stress inhibits distant metastasis by human melanoma cells. *Nature* 2015; **527**:186–191.
11 Ayyasamy V, Owens KM, Desouki MM, Liang P, Bakin A, Thangaraj K, *et al*. Cellular model of Warburg effect identifies tumor promoting function of UCP2 in breast cancer and its suppression by genipin. *PLoS One* 2011; **6**:e24792.
12 Horimoto M, Resnick MB, Konkin TA, Routhier J, Wands JR, Baffy G. Expression of uncoupling protein-2 in human colon cancer. *Clin Cancer Res* 2004; **10**:6203–6207.
13 Derdak Z, Mark NM, Beldi G, Robson SC, Wands JR, Baffy G. The mitochondrial uncoupling protein-2 promotes chemoresistance in cancer cells. *Cancer Res* 2008; **68**:2813–2819.
14 Yu G, Liu J, Xu K, Dong J. Uncoupling protein 2 mediates resistance to gemcitabine-induced apoptosis in hepatocellular carcinoma cell lines. *Biosci Rep* 2015; **35**:e00231.
15 Kawanishi M, Fukuda T, Shimomura M, Inoue Y, Wada T, Tasaka R, *et al*. Expression of UCP2 is associated with sensitivity to platinum-based chemotherapy for ovarian serous carcinoma. *Oncol Lett* 2018; **15**:9923–9928.
16 Li Z. CD133: a stem cell biomarker and beyond. *Exp Hematol Oncol* 2013; **2**:17.
17 Akbari M, Shomali N, Faraji A, Shanehbandi D, Asadi M, Mokhtarzadeh A, *et al*. CD133: an emerging prognostic factor and therapeutic target in colorectal cancer. *Cell Biol Int* 2020; **44**:368–380.
18 Nagata H, Ishihara S, Kishikawa J, Sonoda H, Murono K, Emoto S, *et al*. CD133 expression predicts post-operative recurrence in patients with colon cancer with peritoneal metastasis. *Int J Oncol* 2018; **52**:721–732.
19 Lee JH, Cho YS, Jung KH, Park JW, Lee KH. Genipin enhances the antitumor effect of elesclomol in A549 lung cancer cells by blocking uncoupling protein-2 and stimulating reactive oxygen species production. *Oncol Lett* 2020; **20**:374.
20 Cho YS, Lee JH, Jung KH, Park JW, Moon SH, Choe YS, Lee KH. Molecular mechanism of (18)F-FDG uptake reduction induced by genipin in T47D cancer cell and role of uncoupling protein-2 in cancer cell glucose metabolism. *Nucl Med Biol* 2016; **43**:587–592.
21 Zhang CY, Parton LE, Ye CP, Krauss S, Shen R, Lin CT, *et al*. Genipin inhibits UCP2-mediated proton leak and acutely reverses obesity- and high glucose-induced beta cell dysfunction in isolated pancreatic islets. *Cell Metab* 2006; **3**:417–427.
22 Yin J, Wu M, Li Y, Ren W, Xiao H, Chen S, *et al*. Toxicity assessment of hydrogen peroxide on Toll-like receptor system, apoptosis, and mitochondrial respiration in piglets and IPEC-J2 cells. *Oncotarget* 2017; **8**:3124–3131.
23 Gammon L, Biddle A, Heywood HK, Johannessen AC, Mackenzie IC. Sub-sets of cancer stem cells differ intrinsically in their patterns of oxygen metabolism. *PLoS One* 2013; **8**:e62493.
24 Miwa S, Brand MD. Mitochondrial matrix reactive oxygen species production is very sensitive to mild uncoupling. *Biochem Soc Trans* 2003; **31**:1300–1301.
25 Brand MD, Affourtit C, Esteves TC, Green K, Lambert AJ, Miwa S, *et al*. Mitochondrial superoxide: production, biological effects, and activation of uncoupling proteins. *Free Radic Biol Med* 2004; **37**:755–767.
26 Trachootham D, Alexandre J, Huang P. Targeting cancer cells by ROS-mediated mechanisms: a radical therapeutic approach? *Nat Rev Drug Discov* 2009; **8**:579–591.
27 Tripathi SK, Biswal BK. Piperlongumine, a potent anticancer phytotherapeutic: perspectives on contemporary status and future possibilities as an anticancer agent. *Pharmacol Res* 2020; **156**:104772.
28 Starkov AA. "Mild" uncoupling of mitochondria. *Biosci Rep* 1997; **17**:273–279.
29 Brand MD, Esteves TC. Physiological functions of the mitochondrial uncoupling proteins UCP2 and UCP3. *Cell Metab* 2005; **2**:85–93.
30 Chen C, Yu G, Xiao W, Xing M, Ni J, Wan R, Hu G. Thalidomide inhibits proliferation and epithelial-mesenchymal transition by modulating CD133 expression in pancreatic cancer cells. *Oncol Lett* 2017; **14**:8206–8212.
31 Song Y, Kim IK, Choi I, Kim SH, Seo HR. Oxytetracycline have the therapeutic efficiency in CD133+ HCC population through suppression CD133 expression by decreasing of protein stability of CD133. *Sci Rep* 2018; **8**:16100.
32 Maehara O, Ohnishi S, Asano A, Suda G, Natsuizaka M, Nakagawa K, *et al*. Metformin regulates the expression of CD133 through the AMPK-CEBPβ pathway in hepatocellular carcinoma cell lines. *Neoplasia* 2019; **21**:545–556.